Strain development and damage accumulation during neon ion implantation into silicon at elevated temperatures

C. A. Cima, H. Boudinov, J. P. de Souza, Yu. Suprun-Belevich, and P. F. P. Fichtner

Citation: Journal of Applied Physics **88**, 1771 (2000); doi: 10.1063/1.1305928
View online: http://dx.doi.org/10.1063/1.1305928
View Table of Contents: http://scitation.aip.org/content/aip/journal/jap/88/4?ver=pdfcov
Published by the AIP Publishing

Strain development and damage accumulation during neon ion implantation into silicon at elevated temperatures

C. A. Cima
Programa de Pós-Graduacão em Ciência dos Materiais, Universidade Federal do Rio Grande do Sul, 91501-970, Porto Alegre, R.S., Brazil

H. Boudinov, J. P. de Souza,[a] and Yu. Suprun-Belevich
Instituto de Física, Universidade Federal do Rio Grande do Sul, 91501-970 Porto Alegre, R.S., Brazil

P. F. P. Fichtner
Escola de Engenharia, Universidade Federal do Rio Grande do Sul, 90035-190 Porto Alegre, R.S., Brazil

(Received 15 February 2000; accepted for publication 17 May 2000)

The development of mechanical strain and accumulation of damage in silicon single crystals implanted with Ne ions to doses in the range of $0.1–1.0 \times 10^{17}$ cm^{-2} at temperatures from 200 to 600 °C were investigated employing Rutherford backscattering spectrometry, high resolution x-ray diffraction (HRXRD) analysis and cross section transmission electron microscopy (XTEM). Two distinct layers have been found in the implanted material: A near-surface layer (< 0.2 μm thick) where no extended defects are observed and a buried layer (≈ 0.5 μm thick) containing a dense array of dislocation loops and defect clusters. XTEM analysis revealed a distribution of small spherical cavities presumably filled with Ne, with a diameter <4 nm, extending along the entire depth of the implanted layer. HRXRD studies showed the presence of a positive strain (of expansion), irrespective of the implanted dose and temperature. The findings are discussed in terms of the proposed model which assumes that vacancy-type defects are consumed during the formation of Ne bubbles. © *2000 American Institute of Physics.* [S0021-8979(00)06216-2]

I. INTRODUCTION

Ion implantation of silicon single crystals (*c*-Si) with energetic ions leads to damage production by virtue of the energy transfer from the projectile ions to the lattice atoms. At temperatures where point defects are sufficiently mobile (above ~150 K), recombination of self-interstitials and vacancies produced in the collision cascades anneals out part of the produced damage (dynamic annealing). For temperatures around and below 200 °C the damage accumulates preferentially in regions where a maximum of the ion energy deposition occurs and, depending on the ion dose, an amorphous layer is eventually created. For higher implantation temperatures the dynamic annealing is so intense that an amorphous layer is no longer created even after implantation to high doses ($>10^{17}$ cm^{-2}).

Recently a great deal of interest has been devoted to the high dose and high temperature implantation in *c*-Si, mainly because buried layers of silicon compounds like silicon dioxide, silicon nitride, and silicides can be conveniently prepared by ion beam synthesis.[1] In particular, ion implantation of oxygen ions at elevated temperatures to doses in the range of $0.4–2\times 10^{18}$ cm^{-2} is used in industrial scale for the synthesis of buried silicon dioxide, in the so-called separation by implanted oxygen materials.[2]

It was previously demonstrated that implantation of *c*-Si with Si^+ or O^+ at elevated temperatures leads to formation of two distinct layers: a dislocation free near-surface layer, which presents mechanical strain of contraction, and a highly dislocated layer located around the region of the end of range of the ions.[3–5] This double layer structure appears to be formed due to a spatial separation of point defects formed from the Frenkel pairs in collision cascades.[6] The spatial separation of vacancies and self-interstitials results from the nonzero momentum component of the recoiled Si atoms in the beam incidence direction. As a consequence, in the near surface regions the vacancy concentration exceeds that of the self-interstitials while in regions comprising the end of range of the ions the imbalance in the point defect concentrations reverses. Considering that the dynamic annealing consumes equal concentrations of vacancies and self-interstitials, in the near surface regions vacancy related defects (vacancy clusters) are created while in the regions comprising the end of range of the ions the created defects are interstitial related ones (extrinsic type dislocation loops, stacking faults, clusters of interstitial Si atoms, etc.). The build up of a vacancy cluster distribution in the near-surface layer is responsible for the development of the negative strain (of contraction). On the other hand, the surplus self-interstitial atoms in regions around the end of range of the ions promote the formation of a highly dislocated layer. The role of the impurity atoms in the growth of damage and strain development is not yet clear at present.

Noble gas atoms have negligible solid solubility in *c*-Si. They can be incorporated in silicon as a result of ion beam related processes. Most of the studies were focused on the implantation of Si with He ions. He induced cavities in *c*-Si are very efficient gettering sites for metal impurities, so that He implantation presents potential applications for silicon device technology.[7–9] Implantation of Si with noble gas ions

[a]Electronic mail: souza@if.ufrgs.br

other than He^+ at high temperatures has received little attention up to the present.

In the present article the results of the study of strain and damage accumulation in *c*-Si during Ne^+ implantation at elevated temperatures are presented. It has been found that the developed strain and damage profile in Ne^+ implanted Si markedly contrast with those in *c*-Si implanted with other medium mass ions like N^+, O^+, and Si^+.

II. EXPERIMENT

Czochralski-grown silicon wafers of *n*-type conductivity, with resistivity of 1–2 Ω cm and (100) orientation were implanted with $^{20}Ne^+$ at temperatures of 200, 400, or 600 °C, to doses in the range of $0.1–1.0\times10^{17}$ cm^{-2} at the energy of 140 keV. The beam current density was maintained in the range of 3–6 μA cm^{-2}. In order to minimize channeling effects during the implantation, the normal to the sample surface was tilted by 7° in respect to the incident beam direction and the surface rotated by 25° in respect to the ⟨110⟩ direction.

The as-implanted samples were analyzed by Rutherford backscattering spectrometry (RBS) using an incident beam of 900 keV $^4He^{++}$ in random or in ⟨100⟩ crystal directions. The damage depth profiles were determined from the RBS spectra using an iterative calculation procedure with the two dechanneled beams approximation.[10]

Internal mechanical strain in the samples was investigated by high-resolution x-ray diffraction (HRXRD) measurements in a double-axis configuration using a $Cu\,K\alpha_1$ beam from a Philips 5 crystal diffractometer. To obtain information about the magnitude of the strain and its depth distribution, simulations of the rocking curves were carried out using Philips PC-HRS Simulation and other simulation programs based on the Takagi–Taupin equations of the dynamical theory of diffraction.[11,12] Bragg reflection curves were simulated using various model strain-depth profiles based on known ion and damage profiles, with lattice strain proportional to displaced atom density. By comparing the measured rocking curves with the simulated ones, the corresponding strain $(\Delta d/d)_\perp$ was determined. The in-plane component of the strain was found to be negligible by examination of the reflections from inclined lattice planes.

Cross-section transmission electron microscopy (XTEM) observations were performed at 200 keV using a JEOL 2010 microscope. The XTEM and HRXRD analysis were performed using the facilities of the CME-UFRGS.

III. RESULTS AND DISCUSSION

The damage profiles in the samples implanted at 600 °C to the doses of 0.1, 0.3, and 1.0×10^{17} cm^{-2} are presented in Fig. 1, in curves (a), (b), and (c), respectively. 100% of the damage indicated in the figures corresponds to the ''random level'' or 100% of dechanneling. A layer free of damage (within the sensitivity of the RBS analysis) is observed in regions extending from the surface to a depth of ≈0.15 μm in the sample implanted to the lowest dose (1.0×10^{16} cm^{-2}). The accumulation of the damage occurs in a buried layer which is adjacent to the damage free near-surface layer.

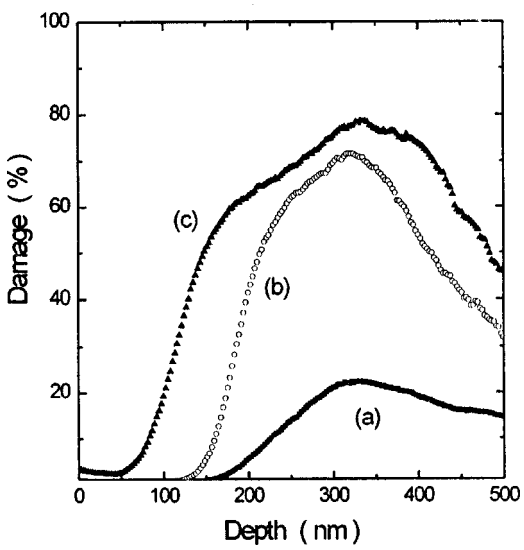

FIG. 1. Damage profiles evaluated from the RBS spectra from Si implanted with 140 keV Ne^+ at 600 °C to the doses of (a) 1.0×10^{16} cm^{-2}, (b) 3.0×10^{16} cm^{-2}, and (c) 1.0×10^{17} cm^{-2}.

In spite of being highly damaged this layer remains single crystalline. The concentration of the damage peaks at the depth of ≈0.32 μm, which practically coincides with the depth of the peak of the Ne concentration profile[13] (0.30 μm). The thickness of this buried damaged layer increases with the Ne^+ dose from ~0.5 μm for the lowest dose [curve (a), dose of 1×10^{16} cm^{-2}] up to ~0.7 μm for the highest dose [curve (c), dose of 1×10^{17} cm^{-2}]. The thickness of the near-surface layer is reduced with the increase of the Ne^+ dose. After the implantation to the highest dose (1.0×10^{17} cm^{-2}) the thickness of the near-surface layer decreases to ≈0.10 μm.

The depth distribution of the damage in the as-implanted samples (evaluated from the RBS spectra) does not correlate well with those reported for O^+ and N^+ implanted *c*-Si.[14] In the case of high temperature O^+ implantation the damage profile practically does not change with the increase of the O^+ dose from 0.3 to 2.0×10^{17} cm^{-2}, indicating saturation of the damage accumulation. In contrast to that, such saturation of the damage accumulation does not occur in the Ne^+ implanted samples since a significant broadening of the damage profile, mostly towards the surface, is observed with the increase of the dose (see Fig. 1).

The rocking curves (RCs) from the samples whose damage profiles are shown in Fig. 1 are displayed in Fig. 2. For the lowest dose (1.0×10^{16} cm^{-2}) the (004) RC consists of a series of thickness fringes with no distinct strain layer peak [see curve (a) in Fig. 2]. The location of the fringes at diffraction angles lower than that of the substrate peak indicates the presence of a positive strain perpendicular to the surface, meaning that the lattice has expanded. RC simulations were also used to evaluate the location of the expanded layer. It was found that there is a strain profile extending from the surface to a depth to 0.6 μm. The strain increases from the surface up to a maximum located at $\cong0.3$ μm and then decreases, vanishing at the depth of $\cong0.6$ μm. Although no distinct fringes are observed on the RC of the higher dose

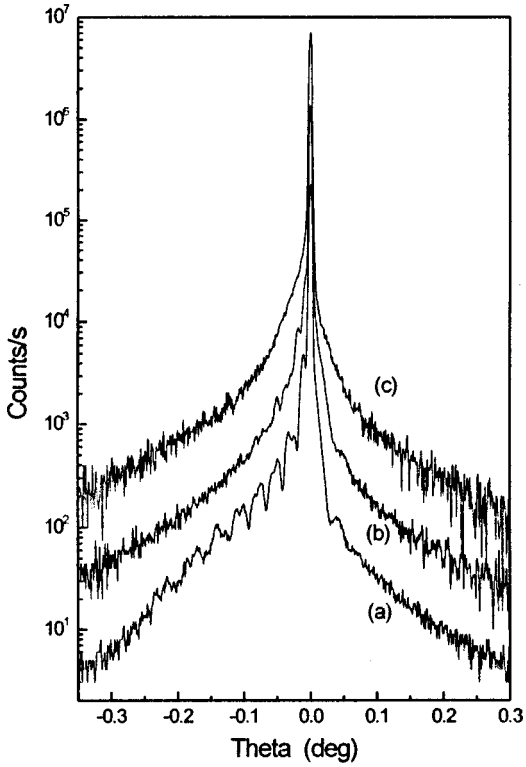

FIG. 2. X-ray rocking curves from Si implanted with 140 keV Ne^+ at 600 °C to the doses of (a) 1×10^{16} cm^{-2}, (b) 3×10^{16} cm^{-2}, and (c) 1×10^{17} cm^{-2}.

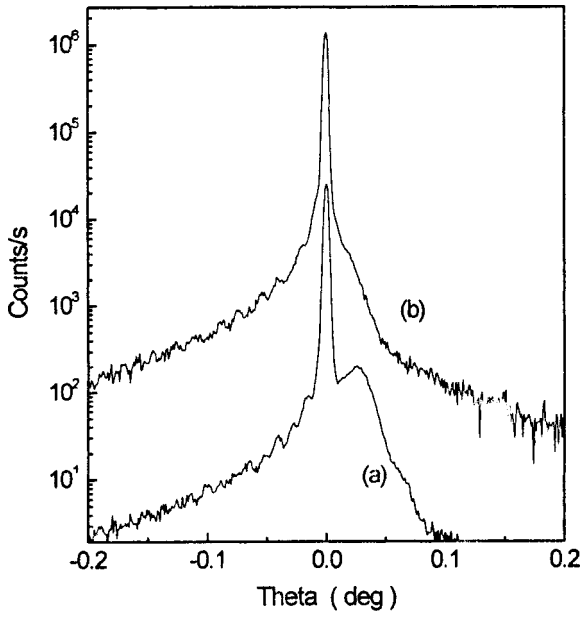

FIG. 3. (a) X-ray rocking curves from Si implanted with 120 keV N^+ to the dose of 1×10^{17} cm^{-2} at 600 °C, and (b) X-ray rocking curve from the sample additionally implanted with 140 keV Ne^+ to the dose of 3×10^{16} cm^{-2} at 600 °C.

cases, the broad shoulder (asymmetry) to the left of the main substrate peak [see curves (b) and (c) in Fig. 2] indicates the presence of a considerable positive strain (of expansion) in the sample.

The behavior of the strain in the Ne^+ implanted samples differs significantly from that in Si implanted with O^+ or N^+. In the case of Ne^+ implantation only the positive strain is observed while in cases of N^+ or O^+ implantation the negative strain develops in the near-surface layer. Negative strain formation is explained by the lattice compression due to an accumulation of vacancy clusters. The accumulation of vacancy-type defects in the near-surface region results from the mechanics of atomic collisions, as discussed above.

The present results clearly indicate that in addition to the ballistic mechanisms, other mechanisms operate during the development of the strain in *c*-Si implanted at high temperatures. It is likely that the efficiency of the formation of the vacancy clusters in the near-surface region during high temperature implantation correlates with the ability of the implanted atoms to form complexes with Si atoms. For example, the implanted N and O atoms produce, respectively, silicon nitride and silicon oxide precipitates embedded in the Si matrix. The open volume in the lattice needed to accommodate the growing precipitate is provided by absorbed vacancies and/or emitted self-interstitial atoms. In regions close to the surface the concentration of impurity atoms is much lower, and consequently the surplus vacancies are free to agglomerate in vacancy clusters which produce the negative strain in the lattice.[5] In the present case (Ne^+ implantation), the implanted species is a chemically inert element, has a negligible solid solubility, and should diffuse rapidly in the Si matrix. These features strongly facilitate the creation of Ne bubbles, even in regions close to the surface. Very likely, the open lattice volume required for the bubble nucleation and growth in the near-surface layer is provided by the local vacancy supersaturation. Using this reasoning one can assume that the formation of the Ne bubbles in the near-surface region consumes vacancies, thus preventing the development of the negative strain and presumably permitting the accumulation of interstitial-type defects (small clusters not visible by TEM). Hence, the small positive strain present in this layer, deducted from the RC simulation, may not result directly from overpressurized Ne bubbles but rather from interstitial-type defects. This point should be further clarified. However, it seems important to remark that, different from the case of He implanted in silicon where overpressurized bubbles may form,[8] the implantation with heavier mass inert gas ions can lead to a damage induced relaxation process which reduces or prevents the build up of the overpressure.[15] Without a significant release of Ne atoms from the samples, the bubbles should achieve thermodynamic equilibrium conditions where the internal gas pressure is compensated by the surface tension of the surrounding matrix, thereby avoiding the appearance of a negative strain.

A separate experiment was performed to obtain further insights into this proposed model. A *c*-Si sample was implanted with N^+ at 600 °C to the dose of 1×10^{17} cm^{-2} at an energy of 120 keV. The HRXRD RC of the N^+ implanted sample is shown in Fig. 3 [curve (a)]. The RC shows a large substrate reflection peak and a secondary peak to the right of the main peak, indicating that there is a layer with negative lattice strain (contraction). The magnitude of the perpendicular strain calculated from the angular difference between the peaks is -6.6×10^{-4}. The sample was subsequently im-

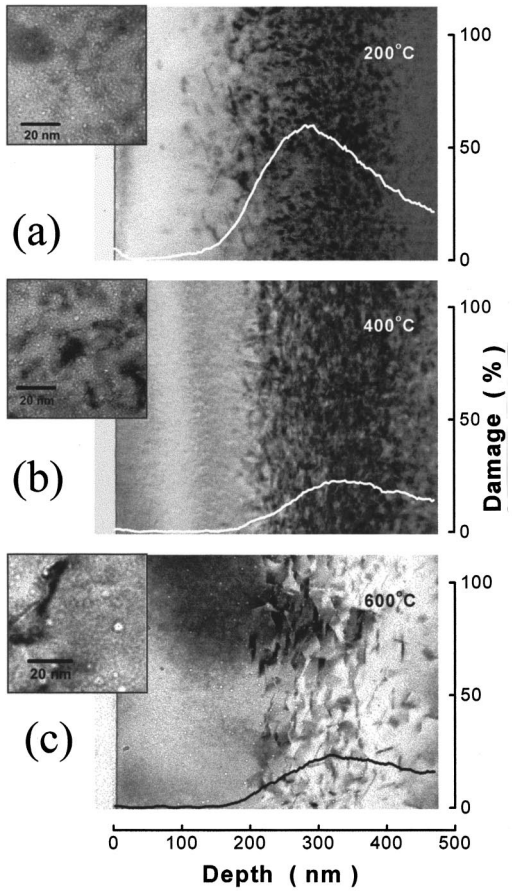

FIG. 4. Cross-section TEM micrographs of Si implanted with 140 keV Ne^+ to the dose of 1×10^{16} cm^{-2} at (a) 200 °C, (b) 400 °C, and (c) 600 °C. The damage depth profiles calculated from the RBS spectra from the same samples are shown superimposed on the micrographs. High magnification cross-section TEM micrographs of the same samples are shown in the insets.

planted with Ne^+ at 600 °C to a dose of 3×10^{16} cm^{-2} at an energy of 140 keV. The RC after the $N^+ + Ne^+$ double implantation clearly demonstrates the suppression of the secondary peak, indicating a significant decrease of the negative strain [see curve (b) in Fig. 5]. The results of this experiment give additional support to the proposed model, suggesting that the vacancy clusters in the near-surface layer are consumed by the developing Ne bubbles.

The structure of the defects created during Ne^+ implantation at a dose of 1.0×10^{16} cm^{-2} was investigated by XTEM. Cross-section micrographs of the samples implanted at 200, 400, and 600 °C are presented in Figs. 4(a)–4(c), respectively. For comparison, the corresponding damage profiles calculated from RBS spectra are displayed over the micrographs.

All three figures show a close correspondence between the depth distribution of the defect structures revealed by TEM and the damage profile calculated from the RBS spectra. A dense dislocation network is observed at depths beyond ≈0.2 μm [see Figs. 4(a)–4(c)] which correlates with the calculated damage in the corresponding curves. Between the surface and the highly dislocated layer the material is dislocation free and this correlates with the negligible damage level close to the surface in the corresponding damage profiles.

In the 200 °C implanted sample, the near-surface dislocation free layer is the thinnest (≈0.10 μm). There is a transition region (from ≈0.10 to 0.20 μm) between the near-surface dislocation free region and the highly dislocated buried layer. In the transition region the densities of dislocation loops and defect clusters increase with the increase of depth. In the 400 and 600 °C implanted samples, the dislocation free near-surface layer is 0.18 and 0.20 μm thick, respectively. With the increase of the implantation temperature from 200 to 400 °C the level of the damage profile decreases significantly [compare Figs. 4(a) and 4(b)]. Besides that, the increase of the implantation temperature leads to the sharpening of the interface between the dislocation free and highly dislocated regions. Furthermore, it was determined from the diffraction mode XTEM analysis that the dislocation loops reside preferentially along the {100} and {110} planes of the Si lattice.

Spherical-like bubbles were observed in the implanted layers from the surface up to the end of range of the ions. In order to make the bubbles easily seen we included high magnification XTEM micrographs in Fig. 4, corresponding to regions around the depth of $\cong0.15$ μm. From the XTEM micrographs the following information regarding the bubble sizes was obtained. At depths from 0.20 to 0.40 μm, the bubble diameters are 2.0 ± 0.6, 2.2 ± 0.6, and 3.5 ± 0.3 nm in the samples implanted at 200, 400, and 600 °C, respectively. In the regions comprising the end of range of the ions the bubble diameters are 1.7 ± 0.2, 1.6 ± 0.2, and 2.5 ± 0.4 nm in samples implanted at 200, 400, and 600 °C, respectively. These data show that the size of the bubbles increases with the implantation temperature. In addition, the bubbles formed in the near-surface region are larger than those around the end of range of the ions.

Figure 5 shows the (004) RCs from the same three samples whose TEM micrographs are presented in Figs. 4(a)–4(c). Irrespective of the implantation temperature, the RCs contain a series of thickness fringes related to an expansion strain but no signs of negative strain were observed. The magnitude of the positive strain perpendicular to the surface estimated from the experimental rocking curves versus the implantation temperature is shown in the inset in Fig. 5. With the increase of the implantation temperature from 200 to 400 °C the strain increases up to 5.4×10^{-3} and then slightly decreases at 600 °C. The strain of expansion is related to the presence of the Ne bubbles, defect clusters, and dislocation loops. At the implantation temperature of 200 °C divacancies should be present in the damaged layer since the annealing of this point defect takes place at a higher temperature of ≈280 °C.[16] Very likely, the divacancies partially compensate the positive strain resulting in the lower strain observed after the 200 °C implantation than that after the implantation at 400 °C. For the 600 °C implantation case, the reduction of strain cannot be explained unambiguously by an eventual coarsening of dislocation loops since the decrease of their density can be compensated by the increase of their average dimension.[17] The decrease of the strain is very likely related to enhancement of the dynamic annealing with tem-

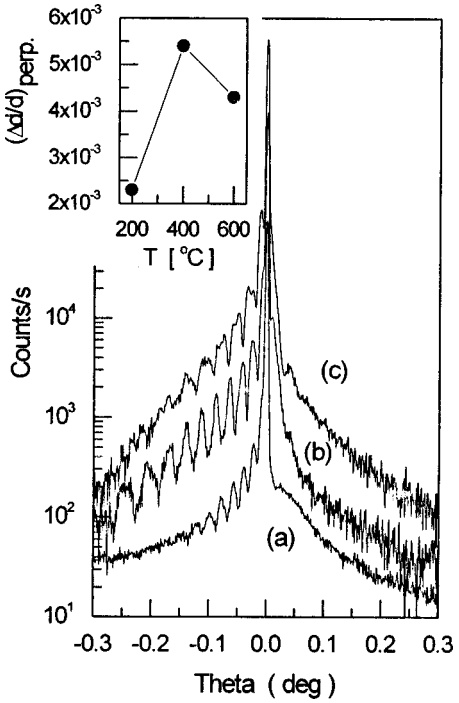

FIG. 5. X-ray rocking curves from Si implanted with 140 keV Ne^+ to the dose of 1×10^{16} cm^{-2} at: (a) 200 °C, (b) 400 °C, and (c) 600 °C.

perature, which should lead to a lower interstitial-type defect content.

The model proposed to explain the lack of negative strain in samples implanted with Ne^+ at high temperatures can be employed to understand the differences in the damage accumulation in Si implanted with Ne and O ions. As discussed above, during O^+ implantation at elevated temperatures, a saturation of the damage accumulation occurs resulting in damage profiles of similar shapes for quite different doses. Such behavior was not observed in the Ne^+ implanted samples (see Fig. 1). In the O^+ implanted samples, a layer with a high concentration of vacancy clusters is formed near the surface. In contrast, in the Ne^+ implants these clusters are absent because the vacancies are consumed by the growing bubbles. During the O^+ implantation the vacancy clusters in the near-surface region prevent the accumulation of self-interstitial atoms, since vacancy related defects play the role of sinks for self-interstitial atoms. However, during the Ne^+ implantation, such sinks are not formed and, consequently, self-interstitial related defects can be formed at a concentration which increases with the Ne^+ dose (see damage profiles in Fig. 1).

IV. CONCLUSIONS

The lattice strain and damage accumulation in Ne^+ implanted silicon at elevated temperatures have been investigated. In contrast to *c*-Si samples implanted with O^+, N^+, or Si^+ at elevated temperatures, where a negatively strained layer is formed near the surface,[3,5,14] in the samples implanted with Ne^+ only a positive strain is observed. In the case of Ne^+ implantation, the ballistic mechanisms which produce an excess concentration of vacancies near the sample surface also take place. However, the implanted Ne atoms diffuse in the Si matrix and agglomerate to create bubbles. Since open spaces in the Si matrix are necessary for nucleation and growth of the bubbles, vacancy related defects should be consumed and/or self-interstitials should be emitted in this process. Consequently, this removing of vacancy related defects during the process of bubble formation may explain the lack of negative strain in the Ne^+ implanted samples. Besides that, it was demonstrated that a high-temperature implantation of Ne^+ into *c*-Si which was previously implanted with N^+ at a high temperature leads to suppression of the negative strain generated by the N^+ implantation. This result gives further indication that the implanted Ne atoms interact with already formed vacancy clusters. Additional Ne^+ co-implantation at a high temperature may be useful to suppress strain in the implanted silicon on insulator structures.

The proposed model can also explain the peculiarities of damage accumulation during high temperature Ne^+ implantation. Since vacancy clusters are not present in the near-surface layer of the samples, self-interstital related defects can be accumulated in the layer during the implantation. The concentration of these defects increases with increase of the Ne^+ dose.

ACKNOWLEDGMENTS

This research was partially supported by Fundação de Amparo à Pesquisa do Estado do Rio Grande do Sul (FAPERGS), Conselho Nacional de Desenvolvimento Científico e Tecnológico (CNPq), and Financiadora de Estudos e Projetos (Finep). The authors are also thankful to the Alexander von Humboldt Foundation, Germany, for donation of the used ion milling apparatus.

[1] O. Almen and G. Bruce, Nucl. Instrum. Methods **11**, 257 (1961).
[2] S. Krause, M. Anc, and P. Roitman, MRS Bull. **23**, 25 (1998).
[3] O. W. Holland, J. D. Budai, and B. Nielsen, Mater. Sci. Eng., A **253**, 240 (1998).
[4] O. W. Holland, D. S. Zhou, and D. K. Thomas, Appl. Phys. Lett. **63**, 896 (1993).
[5] D. Venables, K. S. Jones, F. Namavar, and J. M. Manke, Mater. Res. Soc. Symp. Proc. **235**, 103 (1992).
[6] O. W. Holland and C. W. White, Nucl. Instrum. Methods Phys. Res. B **59/60**, 353 (1991).
[7] S. M. Myers, D. M. Bishop, D. M. Follstaed, H. L. Stein, and W. R. Wampler, Mater. Res. Soc. Symp. Proc. **283**, 549 (1993).
[8] P. F. P. Fichtner, J. R. Kaschny, R. A. Yankov, A. Mücklich, U. Kreißig, and W. Skorupa, Appl. Phys. Lett. **70**, 732 (1997).
[9] W. Skorupa, H. Hatzopoulos, R. A. Yankov, and A. B. Danilin, Appl. Phys. Lett. **67**, 2992 (1995).
[10] F. Eisen, in *Channeling*, edited by D. V. Morgan (Wiley, New York, 1973), p. 417.
[11] S. Takagi, J. Phys. Soc. Jpn. **26**, 1239 (1969).
[12] D. Taupin, Bull. Soc. Fr. Mineral. Cristallogr. **87**, 469 (1964).
[13] J. F. Ziegler, J. P. Biersack, and U. Littmark, in *The Stopping and Range of Ions in Solids* (Pergammon, New York, 1985).
[14] J. P. de Souza, Yu. Suprun-Belevich, H. Boudinov, and C. A. Cima, J. Appl. Phys. **87**, 8385 (2000).
[15] H. Trinkaus, in *Fundamental Aspects of Inert Gases in Solids*, edited by S. E. Donnelly and J. H. Evans (Plenum, New York, 1991) pp. 369–383.
[16] J. W. Corbett, in *Proceedings of the 1st International Conference on Ion Implantation*, edited by L. Chadderton and F. Eisen (Gordon and Breach, New York, 1971), p. 1.
[17] M. A. Krivoglaz, in *X-Ray and Neutron Diffraction in Nonideal Crystals*, (Springer, Berlin, 1996), Chaps. 3 and 4.